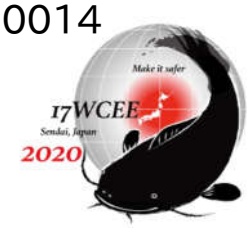

SEISMIC PERFORMANCE OF ABOVE-GROUND LIQUID STORAGE TANKS

E. Brunesi[(1)], A. Pavese[(2)], R. Nascimbene[(3)]

[(1)] *Researcher, European Centre for Training and Research in Earthquake Engineering (EUCENTRE), Pavia, Italy,* emanuele.brunesi@eucentre.it

[(2)] *Associate Professor, Department of Civil Engineering and Architecture (DICAr), University of Pavia, Pavia, Italy,* a.pavese@unipv.it

[(3)] *Researcher, European Centre for Training and Research in Earthquake Engineering (EUCENTRE), Pavia, Italy,* roberto.nascimbene@eucentre.it

Abstract

Past seismic events have repeatedly shown the vulnerability of above-ground liquid storage steel tanks, demonstrating the need to properly design them to mitigate their potential for damage due to seismic actions. Amongst others, one important damage mechanism in these plant items, which serve a vast variety of purposes involving the extraction and distribution of raw or refined materials, often inflammable and/or pollutant, is the dynamic buckling of the tank's walls. This paper presents and proposes a numerical framework to evaluate the earthquake-induced hydrodynamic pressures acting on the walls of cylindrical steel tanks as a result of the inertial forces generated during earthquake excitation. The computational framework takes into account material and geometrical nonlinearities in the tank, which was modelled by 4-noded, 2-points integration, Belytschko shell elements, and makes use of the Arbitrary Lagrangian Eulerian method to allow for large structural and liquid deformation, thus implying that fluid-structure interaction could be fully reproduced through highly nonlinear algorithms. Experimental test data were used to validate the assumed modelling approach and to simulate sloshing phenomena as well as stress concentrations in the tank's walls that cause them to buckle. Results of parametric analysis undertaken by varying the height-to-radius ratio and the radius-to-thickness ratio of a representative anchored flat-bottomed tank were discussed to examine the seismic performance of such a widely used storage system, providing a paradigm that relates tank's properties and mechanical behaviour under dynamic loading.

Keywords: liquid storage tanks, earthquake-induced actions, dynamic buckling, tank's wall, numerical modelling

© The 17th World Conference on Earthquake Engineering

1. Introduction

Cylindrical steel tanks are common storage systems, widely used in many industrial applications, since they represent a basic strategic component employed in several plants for the containment and exploitation of different types of materials such as water, oil, nitrogen, high-pressure gas, and petroleum or other hazardous chemical substances. As such, fire and fluid spillover are main concerns because they may cause both direct and indirect losses, leading for instance to irreparable environmental pollution. As evidenced by the 2012 Emilia earthquakes [1-3], the exposure of these shell structures, in combination with their intrinsic structural deficiencies, made them disproportionately vulnerable to these events, even in the case of moderate seismic intensity. Severe damages have caused the majority of them to be out of service in the aftermath of the 2012 Emilia seismic sequence and the subsequent interruption of the industrial production in the stricken area has been estimated to produce an economic loss of approximately 5 billion Euros.
The significant number of storage structures surveyed have revealed failure mechanisms already shown by destructive earthquakes in other regions [4-8], thus confirming the poor performance of these systems, typical of the past design practice, when put to test by seismic events. The prevailing types of collapse modes encountered during reconnaissance were elephant's foot and diamond buckling induced by hydrodynamic pressures as a result of inertial forces imparted under seismic excitation, as well as the fracture of anchors. Examples of these failure mechanisms are collected in Figure 1 and Figure 2. In particular, Figure 1(a-c) report typical cases of classical elephant's foot buckling developed, in flat-base tanks, as a consequence of the combination of large circumferential tensile stresses induced by internal hydrostatic and hydrodynamic pressures and the axial compression due to the overturning moment caused by the horizontal seismic loads. Diamond-shaped buckling mechanisms at the base of the wall (see Figure 1(d) and Figure 1(e)) or in correspondence of the circumferential welds, concomitantly with the reduction of the wall thickness along the height, was another very common occurrence observed for such flat-bottomed cylindrical steel tanks (see Figure 1(f)).

Fig. 1 - (a-c) Elephant's foot and (d-f) diamond-shaped buckling mechanisms observed in the aftermath of the May 2012 Emilia seismic sequence

Examples of base-anchorage failures, in flat-base or leg-supported systems, are provided in Fig. 2. In some cases, this mechanism was associated with an elastic diamond-shaped buckling of the tank wall (see Figure 2(a)), but it was more frequently observed to occur independently, as a consequence of the excessive inelastic strain demands exerted in the anchor bolts, which caused their fracture or debonding from the concrete pads. Another anchoring system-related mode, shown in Figure 2(b), was a prominent spalling of concrete due to its low resistance. Therefore, these flat-bottomed systems, poorly anchored and detailed to sustain any earthquake-induced demand, failed in tension in the weakest link of their anchoring system, as a consequence of sliding and rocking of the tank. Finally, Figure 2(c) and Figure 2(d) present a typical example of the shear-buckling mechanism observed in legged tanks. In detail, the coupling between heavy

© The 17th World Conference on Earthquake Engineering

static loads and the effect of horizontal and vertical seismic excitation resulted into prominent stress/strain concentrations at the base of the stocky legs, where their resistance is lower. This made them slide, after failure of the anchorage, and, then, visibly buckle, being the verticality of the tank lost. By contrast, these systems performed considerably better, if unanchored, since they were found to rock and slide relatively to the ground. When the piping system was flexible enough to accommodate seismic displacements and the legs were strong enough to rock, no damage in the tank or falling off their foundation was observed.

Fig. 2 - Anchoring system-related modes experienced in (a-b) flat-base and (c-d) leg-supported storage tanks during the May 2012 Emilia seismic sequence: (a) fracture of anchors and (b) concrete spalling at the anchorage; (c-d) loss of verticality due to shear-buckling in stocky tapered legs

Field observations following the May 2012 Emilia earthquakes have reaffirmed the complex dynamic response of such liquid storage tanks, mostly designed as thin shells to resist the hydrostatic pressure exerted when filled, without any additional seismic requirement and/or detailing demanded in current major Codes [9-17]. Dynamic buckling mechanisms, which are currently recognised to be a crucial aspect in the design of these structures because of the small thicknesses of their walls, were only accounted for by empirical closed-form expressions or prevented by mere concepts of good-design-practice available at that time, thus providing inadequate protection against earthquakes. Furthermore, the crucial contribution of wall flexibility was generally omitted in the design process, something that calls for high-definition/fidelity modelling of the fluid-structure interaction and for nonlinear dynamic analyses that simulate the hydrodynamic response of the liquid-tank system over time under earthquake-induced actions.

2. Numerical Modelling

Nowadays, several computational strategies, involving mechanics-based surrogate modelling or sophisticated fluid-structure interaction algorithms, can be used to reproduce the complex response of above-ground liquid storage structures, whose behaviour is driven by a combination of many interacting phenomena. Beginning with the seminal studies by Jacobsen [18] and Housner [19] among others, the response of tanks subjected to a dynamic excitation has been pioneered and described in terms of La Place's equation, which assures the conservation of mass and momentum in the liquid-structure system – note that the solution to this equation assumes the liquid to be incompressible, inviscid and irrotational. Since those times, many researchers (see e.g. Veletsos et al. [20], Chen et al. [21], Malhotra [22]) have continued to add or elaborate, simplifying the abovementioned seminal formulation. On the other hand, a significant number of research efforts have demonstrated the feasibility of more detailed finite element (FE) procedures and methodologies over the last

© The 17th World Conference on Earthquake Engineering

three decades (among others, see [23-26]). FE-based models implemented with either added-mass approximations [3, 25] or fluid-specific capabilities [26, 27], BE-FE coupled models [24] and smoothed particle hydrodynamics [23], have been explored in the literature. Even though liquid modelling-related simplifications have been introduced in many early studies, more recent contributions explicitly incorporate fluid-structure interaction in the most accurate way, adopting Lagrangian, Eulerian, and Lagrangian-Eulerian formulations. To name few examples, Sezen et al. [26] assumed a displacement-based Lagrangian approach, while Ozdemir et al. [27] made use of the Arbitrary Lagrangian Eulerian (ALE) formulation to simulate the liquid-wall interaction in anchored and unanchored tanks.

In light of this, high-definition FE analyses appear an attractive tool for seismic response assessment of such structures, as they are able to reproduce not only their global behaviour but also stress/strain concentrations, crucial in interpreting damage patterns and failure modes. Therefore, a series of detailed FE models have been developed and nonlinear dynamic analyses, including nonlinear sloshing effects as well as geometrical and material nonlinearities, have been performed using the general-purpose FE package with fluid-structure interaction capabilities LS-DYNA [28]. An ALE algorithm based on the arbitrary movement of a referential domain, which is introduced as a third domain in addition to the common material (Lagrangian) domain and spatial (Eulerian) domain, has been considered here to allow for large structural and liquid deformation. The penalty coupling method for shell and solid that falls within the CONSTRAINED_LAGRANGE_IN_SOLID framework has been assumed to behave in compression only, and the compressible Navier-Stokes equations have been selected to describe the motion of the fluid. The latter has been modelled by a mesh of 8-noded, 1-point integration ALE solid elements. In order to model both base plate and walls of the case study tanks, 4-noded, 2-points integration shell elements, in accordance with the formulation proposed by Belytschko et al. [29], have been used, since they are a computationally efficient solution based on a combined co-rotational and velocity-strain formulation. Bilinear elastic-plastic constitutive law (MAT_003), with a combination of isotropic and kinematic hardening, has been assumed to reproduce any eventual permanent deformations exhibited by the tank wall under seismic excitation. Null material has been selected for the fluid that, in this paper, is chosen to be water, thus implying a bulk modulus of $2.25 \cdot 10^9$ N/m^2. In addition, the anchored flat-bottomed case study tanks have been analysed as completely filled, which is not only the most common but also the most demanding operation condition for such storage systems. An explicit solution strategy has been employed to carry out all nonlinear dynamic simulations with an automatic mesh-dependent integration time step of the order of 10^{-6}.

Such a detailed numerical approach able to account for many sources of nonlinearity, such as large amplitude nonlinear sloshing of free surface liquid and yielding/buckling mechanisms of the tank wall, has firstly been applied to predict the experimental response of two small-scale tank specimens [30, 31], as described in what follows.

3. Experimental Validation

The first tank specimen is the one tested in the pioneering experimental research by Manos and Clough [30]. More in detail, an open-top, anchored tank resting on rigid foundation was analysed numerically. The tank prototype used in the experiments was a 1/3 scaled structure having radius of about 1.83 m and height of 1.83 m. The system was filled with water up to a height of 1.53 m. The tank was made of aluminum with a density of 2700 kg/m^3. The thickness of the base plate was 2 mm. The same thickness was used for the tank wall, which however has a second course with a thickness equal to 1.3 mm. An L-shaped steel girder was placed onto the top of the second shell course. In the shake-table test, the input motion was derived from the horizontal component of the El Centro 1940 earthquake assuming a peak ground acceleration of 0.50g. The input was then scaled with respect to time by a factor equal to $1/(3)^{0.5}$ because of similitude requirements.

Figure 3 shows a schematic of the small-scale tank specimen tested, along with key geometrical information, whereas the FE model developed for numerical simulation is presented in Figure 4. It is noted that the model consisted of 5793 nodes, 890 shell elements and 4320 solid elements, and that a single nonlinear transient simulation took more than 15 hours to be completed.

© The 17th World Conference on Earthquake Engineering

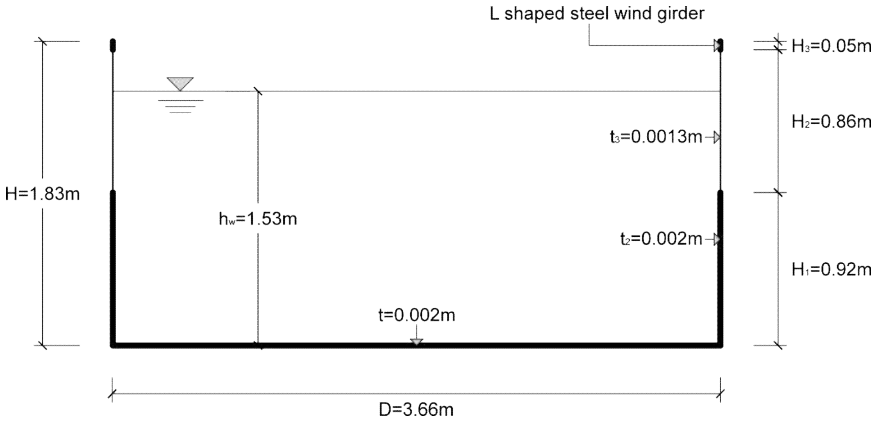

Fig. 3 - Dimensions and characteristics of the small-scale tank specimen tested by Manos and Clough [30]

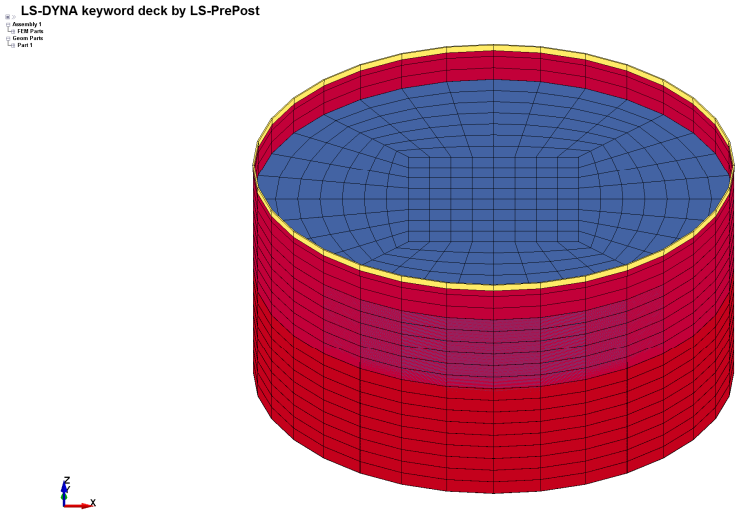

Fig. 4 – High-definition FE model developed to simulate shake-table test results [30]

A comparison between numerical predictions and experimental test data is given in terms of pressure time-history at different locations up to the height of the tank wall, as shown in Figure 5. Numerical predictions are in close correlation with experimental results, as almost negligible differences can be observed. Response graphs reveal that the pressure peaks were predicted in a very consistent and accurate manner, and the same applies to the post-peak response of the analysed tank specimen. Similar considerations can be drawn for the shape and amplitude of sloshing wave, as small discrepancies (<5%) stem from the comparison between the numerical data and the experimental results obtained by Manos and Clough [30].

The aforementioned numerical techniques were considered to predict the experimental response of another tank specimen, which is the one tested by Haroun [31]. In particular, this cylindrical tank is an open-top, anchored, small-scale prototype filled with water. The tank wall was made of aluminum with density of 2600 kg/m^3. The radius of the tank was 1.18 m; its total height was 4.57 m, whilst the height of the water free surface was 3.96 m. The 1994 El Centro earthquake, scaled to a PGA equal to 0.5 g, was assumed by Haroun [31] to perform the shake-table test considered here for validation purposes. Due to the scaling of the model, the record has been speeded up by a 1.73 factor and has been scaled by 1.43 so as to obtain a peak ground acceleration of 0.5g. In this case, 1236 two-dimensional shell elements have been used to mesh the base plate and the wall, while the fluid portion has been modelled by means of 6084 three-dimensional solid elements with ALE formulation. The total number of nodes of the FE model is 8009.

Figure 6 presents the deformed shape of the model at different time instants, whereas the prevailing results obtained numerically are collected in Table 1. Also in this case, numerical predictions are in close agreement

© The 17th World Conference on Earthquake Engineering

with experimental results, as a difference of about 2% was indeed obtained in terms of maximum base shear. Similar discrepancies were also observed as far as the maximum meridional compressive force and the peak radial displacement are concerned.

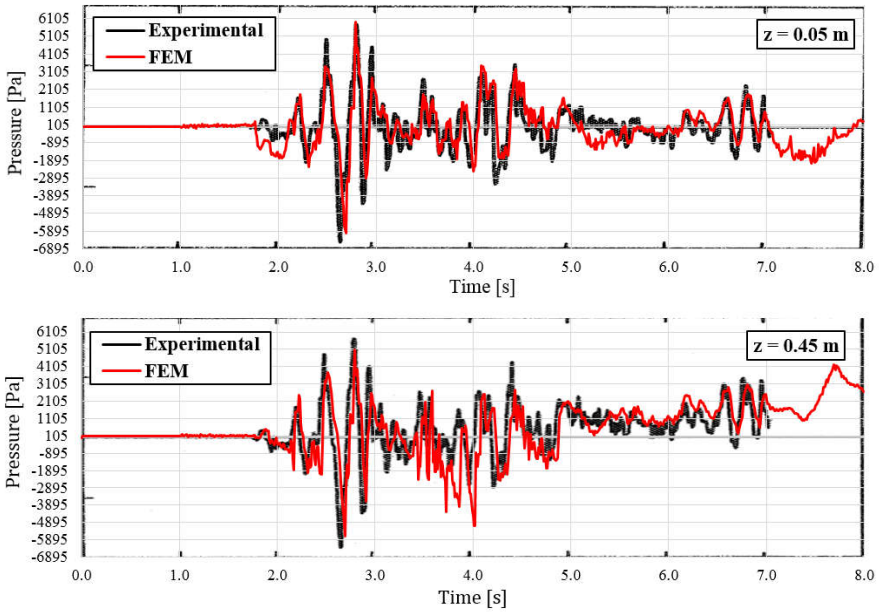

Fig. 5 - Comparison between numerical and experimental [30] pressure time histories

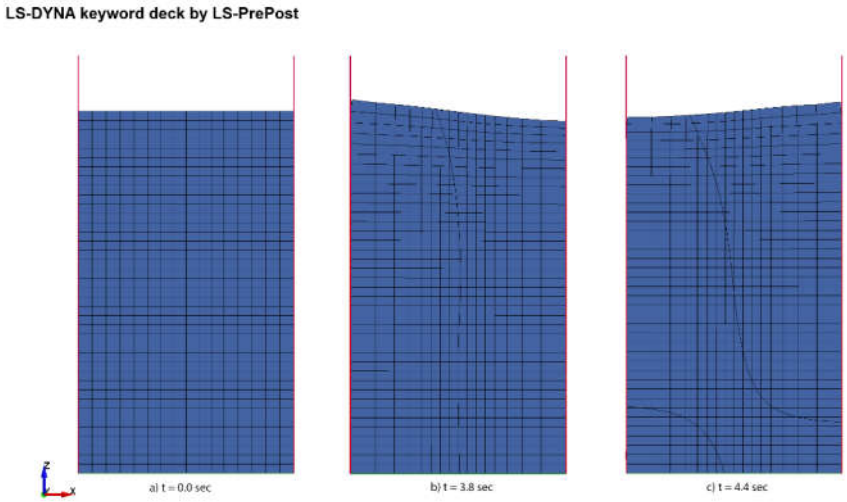

Fig. 6 - FE model for simulation of shake-table test results by Haroun [31] and deformed shape at different time instants during explicit nonlinear dynamic analysis

Table 1 – Comparison between experimental [31] and numerical results

Parameter	Experimental	LS-DYNA	[%]
Max Radial Displacement (shell top) [mm]	3.32	3.40	2.41
Max Meridional Compression [N/m]	63396	62205	1.88
Max Base Shear [kN]	122	125	2.46

© The 17th World Conference on Earthquake Engineering

4. Parametric analyses of selected tanks

Once the aforementioned numerical techniques were validated in compliance with experimental test data [30, 31], two sets of parametric FE analyses have been performed to explore the seismic response of these liquid storage systems considering different ground motion records, as explained hereafter.
The first series of dynamic simulations have been carried out assuming the most severe ground motion of the two horizontal components recorded in the station closest to the epicenter of the May 20th Emilia earthquake (i.e. North-South component – see NS MRN of Figure 7 for the spectral characteristics of this record). Note that the acronym/Code MRN stands for Mirandola Station, and that, in Figure 7, the spectral demands from the two time histories recorded at that station are compared with the spectral shapes computed according to the Italian building code for different return periods.

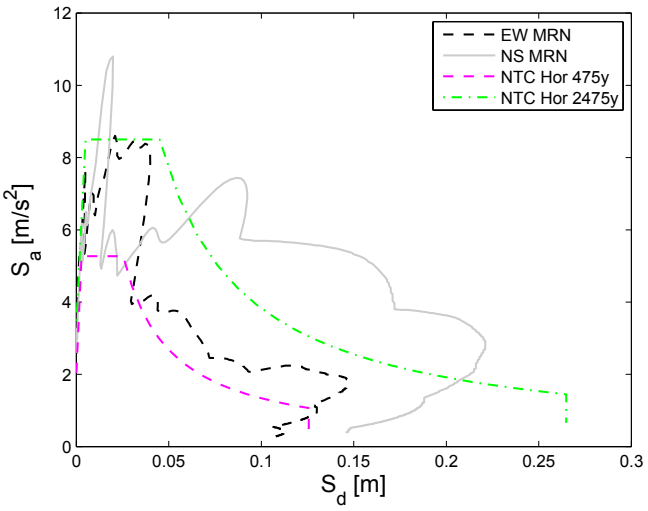

Fig. 7 - Elastic acceleration displacement response spectra from recorded time histories at MRN station (NS and EW) and in accordance with the Italian building code

Numerical predictions are collected and presented in Figure 8 to point out behavioral changes in the seismic response of storage tanks as a consequence of variations in their geometrical characteristics. More in detail, the selected prototype tanks are characterised by different values of both height-to-radius ratio (*H/R*) as well as radius-to-thickness ratio (*R/t*).

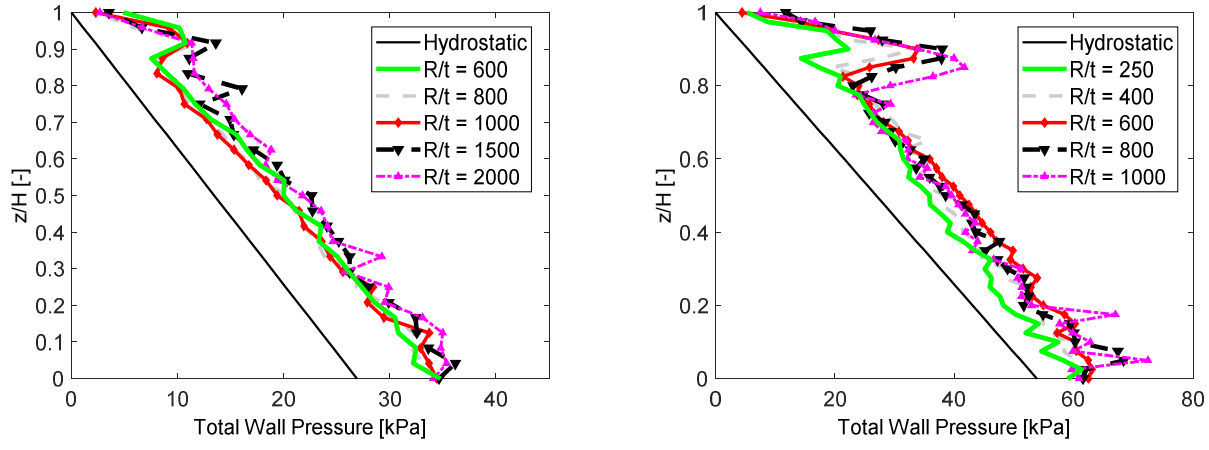

(a) (b)

Fig. 8 - Total wall pressure distribution along the height for (a) *H/R* = 1.5 and (b) *H/R* = 3.0

© The 17th World Conference on Earthquake Engineering

Figure 8(a) presents the pressure peak profiles obtained for five medium-size tanks (H/R = 1.5) with varying R/t, whereas the counterpart information for relatively slender tanks (H/R = 3.0) can be found in Figure 8(b). As far as the former set of tank prototypes is concerned, the radius-to-thickness ratio was set to be in the 600-2000 range, whilst $250 \leq R/t \leq 1000$ for the latter set of liquid storage tanks. It can be seen from Figure 8 that medium-size tanks tend to show a relatively uniform pressure peak profiles, with moderate concentrations at the top of the shell that become more pronounced for higher R/t ($R/t \geq 1500$). This effect, associated with the sloshing motion of the liquid, is clearly more significant for slender tanks, as can be observed in Figure 8(b). In addition, it can be reaffirmed from therein that the pressure concentrations increase as R/t increases. Such trend becomes evident for R/t equal to or larger than 400, as in these cases the pressure peak profile assumes an approximately linear piecewise decaying slope with the tank height (or the normalised tank height).
The second set of parametric FE analyses have been performed assuming a suite of ten natural records scaled by Maley et al. [32] to obtain displacement spectrum compatibility according to EC8 requirements [33]. The acceleration and displacement response spectra shown in Figure 9 correspond to EC8 type 1 spectra for a peak ground acceleration of 0.40g and soil type C, but with T_D equal to 8s such that spectral displacement demands increase linearly up to this value of corner period. Further and more comprehensive information concerning the prevailing criteria assumed for this set of accelerograms, originated from earthquakes ranging in magnitude from 6.2 to 7.6, may be found in Maley et al. [32].

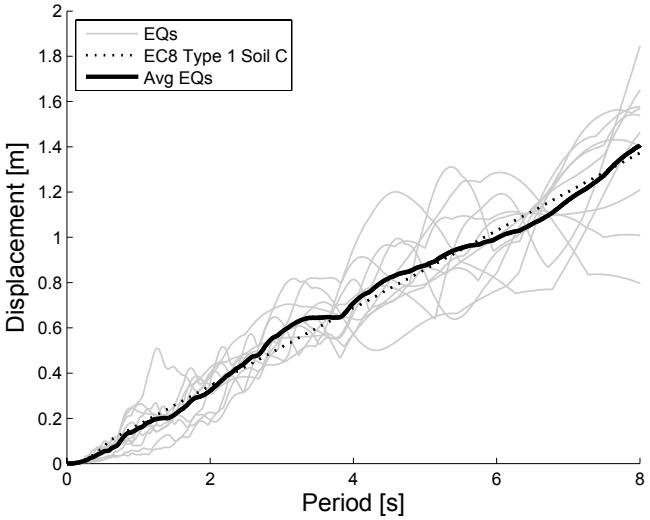

Fig. 9 - Elastic displacement response spectra from ground motion records selected by Maley et al. [32]

Three additional anchored flat-bottomed (AFB) tanks involving broad, medium and slender geometries have been selected and designed, resulting in the following configurations: (i) T1b – H/R = 0.75 and R/t = 2000, (ii) T2m – H/R = 1.5 and R/t = 400, and (iii) T3s – H/R = 4 and R/t = 400. Figure 10 shows the pressure peak profiles obtained for each AFB case-study tank, in terms of individual profile for each record resulting from explicit nonlinear transient analysis as well as the calculated mean and mean plus one standard deviation.
As can be seen from Figure 10(a), broad tanks are much less affected by sloshing phenomena – than medium and slender tanks – and show a fairly linear decaying slope of total wall pressure with concentrations that are observed to occur at the bottom of the shell. The total wall pressure increases as H/R increases and nonlinear sloshing effects become more pronounced, as highlighted by Figure 10(b) and Figure 10(c). It is noteworthy that concentration of pressures acting on the tank walls are observed to take place both at top and bottom of the shell for tank T2m – see Figure 10(b). Sloshing-related damage is predicted to occur in tank T3s, since in some cases very high concentration of pressures are found to take place at the top of the shell.
The above trends are also reflected in Figure 11, where the mean peak pressure profiles along with the mean plus one standard deviation counterparts are presented and compared together.

© The 17th World Conference on Earthquake Engineering

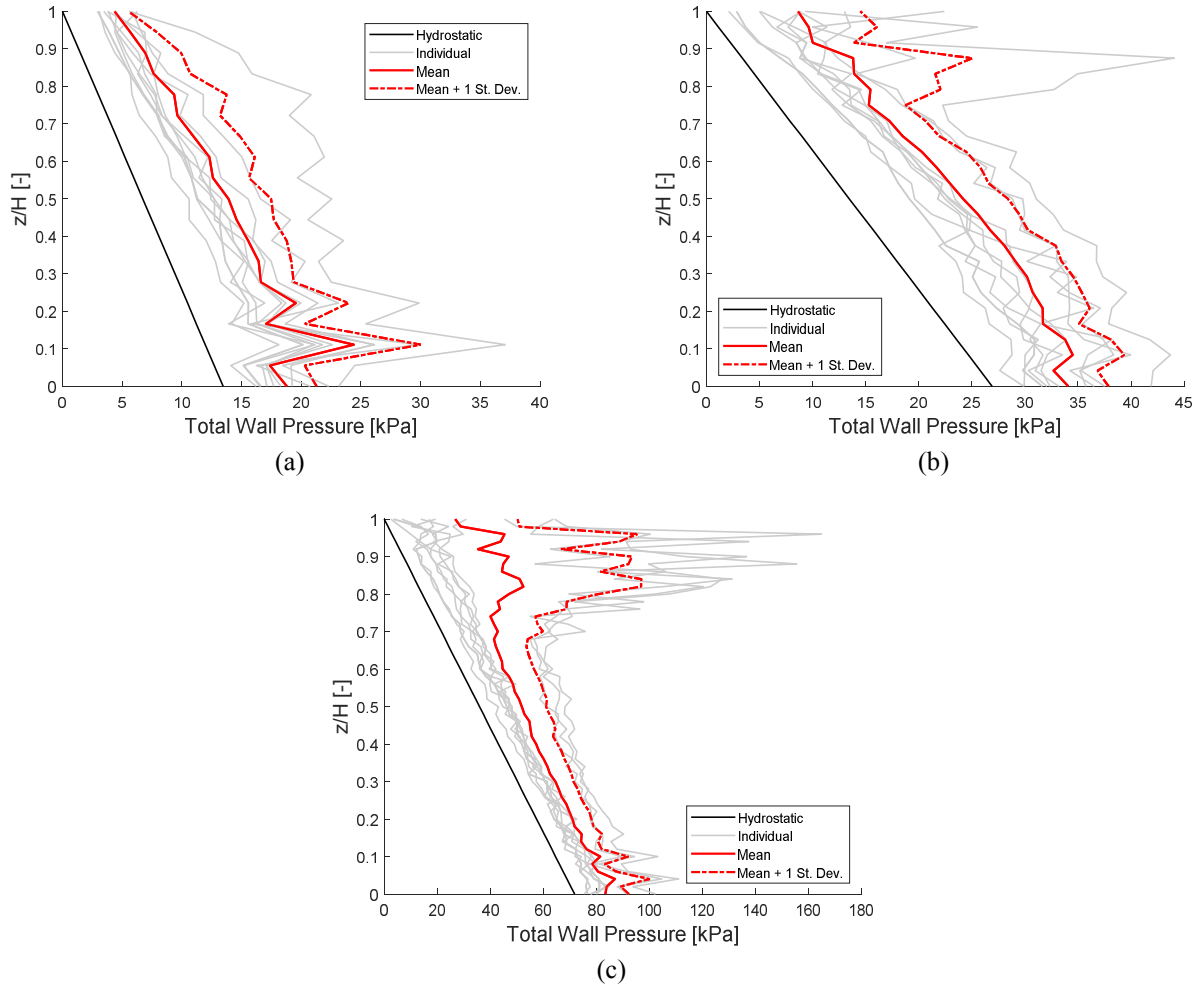

Fig. 10 - Wall pressure peak profiles (individual records, mean and mean plus one standard deviation) for (a) $H/R = 0.75$ and $R/t = 2000$, (b) $H/R = 1.5$ and $R/t = 400$, and (c) $H/R = 4$ and $R/t = 400$

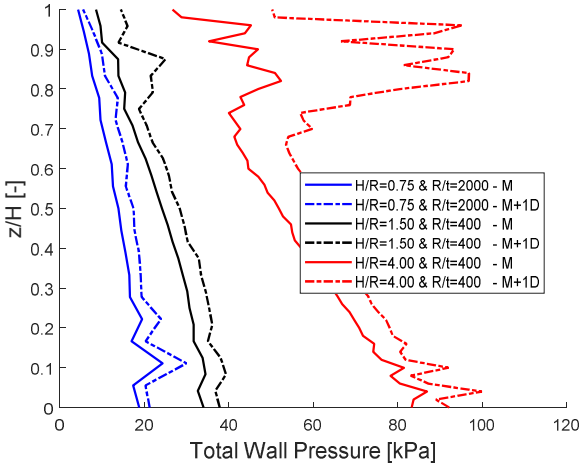

Fig. 11 – Comparison between wall pressure peak profiles (mean and mean plus standard deviation)

© The 17th World Conference on Earthquake Engineering

5. Conclusions

The work described herein investigates the seismic response of above-ground liquid storage steel tanks, in light of field observations collected in the aftermath of the May 2012 earthquakes in Northern Italy. Despite the moderate ground motion intensity [half of the Italian Territory is indeed exposed to values of hazard equal or higher than the value computed for the epicentral area], the vast majority of them suffered excessive damage, which led to substantial direct and indirect losses. Their poor performance is mainly motivated by a significant delay in the adoption and implementation of adequate seismic provisions, resulting in lack of design and detailing. The prevailing types of failure, including elephant's foot and diamond-shaped buckling of thin shell walls, as well as base-anchorage and tank support-system failures, have been collected and called for a series of detailed FE analyses. All geometrically and materially nonlinear numerical models have been developed by making use of a general-purpose FE package with fluid-structure interaction capabilities.
The fully nonlinear dynamic numerical procedure proposed in this paper relies upon the ALE formulation to allow large structural and liquid deformation and is able to account for many sources of nonlinearity, such as large amplitude nonlinear sloshing of free surface liquid and yielding/buckling mechanisms of the tank wall. Its effectiveness and accuracy have been tested by reproducing the experimental response of two small-scale tank specimens. Comparison between test data and numerical results served as a validation of this modelling approach, which was then used to perform a set of explicit nonlinear dynamic simulations aimed at exploring behavioural changes in the seismic response of AFB tanks as a consequence of parametric variations in their geometry, namely H/R and R/t. Results of two series of parametric analyses have been discussed to examine the seismic performance of this commonly used liquid storage system, providing a paradigm that relates tank properties and mechanical behaviour under dynamic loading.
Thus, the modelling and numerical outcome of this research is directly applicable to design, assessment, and strengthening of such vulnerable structures. The numerical results shown here suggest the need for analysis and proposal of efficient retrofit solutions for cost-effective mitigation/prevention of further failures due to earthquake-induced actions. Recommendations for earthquake-resistant strengthening methodologies, acting on the performance of structural components as well as on that of the structure as a whole, are currently the focus of ongoing research.

6. Acknowledgements

This study was developed within the activities of the Eucentre-DPC 2019-2021 research program, WP15 "Piattaforma Web-GIS per il calcolo del rischio sismico, degli scenari di danno e dell'effetto di danni in cascata su insediamenti chimici industriali". The authors would like to express their gratitude to the Italian Department of Civil Protection for the financial support received through a three-year framework program established with the European Centre for Training and Research in Earthquake Engineering.

7. References

[1] Luzi L, Pacor F, Ameri G, Puglia R, Burrato P, Massa M, Augliera P, Franceschina G, Lovati S, Castro R (2013): Overview of the strong-motion data recorded during the May-June 2012 Emilia seismic sequence. *Seismological Research Letters*, **84**(4), 629-644.

[2] Brunesi E, Nascimbene R, Pagani M, Beilic D (2015): Seismic performance of storage steel tanks during the May 2012 Emilia, Italy, earthquakes. *Journal of Performance of Constructed Facilities*, **29**(5), 04014137.

[3] Buratti N, Tavano M (2014): Dynamic buckling and seismic fragility of anchored steel tanks by the added mass method. *Earthquake Engineering and Structural Dynamics*, **43**(1), 1-21.

[4] Manos G (1991): Evaluation of the earthquake performance of anchored wine tanks during the San Juan, Argentina, 1977 Earthquake. *Earthquake Engineering and Structural Dynamics*, **20**(12), 1099-1114.

[5] Niwa A, Clough R (1982): Buckling of cylindrical liquid-storage tanks under earthquake loading. *Earthquake Engineering and Structural Dynamics*, **10**(1), 107-122.

© The 17th World Conference on Earthquake Engineering

[6] Swan W, Miller D, Yanev P (1984): The Morgan hill earthquake of April 24, 1984 - effects on industrial facilities, buildings, and other facilities. *Earthquake Spectra*, **1**(3), 457-568.

[7] Zareian F, Sampere C, Sandoval V, McCormick DL, Moehle J, Leon R (2012): Reconnaissance of the Chilean Wine Industry Affected by the 2010 Chile Offshore Maule Earthquake. *Earthquake Spectra*, **28**(S1), 503-512.

[8] González E, Almazán J, Beltrán J, Herrera R, Sandoval V (2013): Performance of stainless steel winery tanks during the 02/27/2010 Maule Earthquake. *Engineering Structures*, **56**, 1402-1418.

[9] CEN, European Committee for Standardisation. *ENV 1998-4, Eurocode 8: Design of structures for earthquake resistance – Part 4: Silos, tanks and pipelines*. Brussels, Belgium, 2006.

[10] UNI EN 14015. *Specification for the design and manufacture of site built, vertical, cylindrical, flat-bottomed, above ground, welded steel tanks for the storage of liquids at ambient temperature and above*, CEN – European Committee for Standardization. Brussels, Belgium, 2006.

[11] NZSEE. *Recommendations for seismic design of storage tanks*. New Zealand National Society for Earthquake Engineering, 2009.

[12] ACI 350.3-06. *Seismic design of liquid containing structures and commentary*. American Concrete Institute, Farmington Hills, MI, 2006.

[13] API 620. *Design and construction of large, welded, low-pressure storage tanks*. American Petroleum Institute Standards, Washington, DC, 2012.

[14] API 650. *Welded steel tanks for oil storage*. American Petroleum Institute Standards, Washington, DC, 2012.

[15] AWWA D100. *Welded carbon steel tanks for water storage*. American Water Works Association, Denver, CO, 2011.

[16] AWWA D103. *Factory-coated bolted carbon steel tanks for water storage*. American Water Works Association, Denver, CO, 2009.

[17] AIJ. *Design recommendation for storage tanks and their supports with emphasis on seismic design*. Architectural Institute of Japan, Tokyo, Japan, 2010.

[18] Jacobsen LS (1949): Impulsive hydrodynamics of fluid inside a cylindrical tank and of fluid surrounding a cylindrical pier. *Bulletin of the Seismological Society of America*, **39**(3), 189-204.

[19] Housner GW (1957): Dynamic pressures on accelerated fluid containers. *Bulletin of the Seismological Society of America*, **47**(1), 15-35.

[20] Veletsos AS, Tang Y, Tang HT (1992): Dynamic response of flexibly supported liquid-storage tanks. *Journal of Structural Engineering*, **118**(1), 264-283.

[21] Chen W, Haroun MA, Liu F (1996): Large amplitude liquid sloshing in seismically excited tanks. *Earthquake Engineering and Structural Dynamics*, **25**(7), 653-669.

[22] Malhotra PK (2000): Practical nonlinear seismic analysis of tanks. *Earthquake Spectra*, **16**(2), 473-492.

[23] Gingold RA, Monaghan JJ. Kernel estimates as a basis for general particle methods in hydrodynamics. Journal of Computational Physics 1982; 46(3): 429-453.

[24] Kim MK, Lim YM, Cho SY, Cho KH, Lee KW (2002): Seismic analysis of base-isolated liquid storage tanks using the BE-FE-BE coupling technique. *Soil Dynamics and Earthquake Engineering*, **22**(9-12), 1151-1158.

[25] Virella JC, Godoy LA, Suárez LE (2006): Dynamic buckling of anchored steel tanks subjected to horizontal earthquake excitation. *Journal of Constructional Steel Research*, **62**(6), 521-531.

[26] Sezen H, Livaoglu R, Dogangun A (2008): Dynamic analysis and seismic performance evaluation of above-ground liquid-containing tanks. *Engineering Structures*, **30**(3), 794-803.

[27] Ozdemir Z, Souli M, Fahjan YM (2010): Application of nonlinear fluid-structure interaction methods to seismic analysis of anchored and unanchored tanks. *Engineering Structures*, **32**(2), 409-423.

[28] Hallquist JO (2006): *LS-DYNA keyword user's manual*. Livermore Software Technology Corporation.

© The 17th World Conference on Earthquake Engineering

[29] Belytschko T, Lin JI, Tsay CS (1984): Explicit algorithms for the nonlinear dynamics of shells. *Computer Methods in Applied Mechanics and Engineering*, **42**(2), 225-251.

[30] Manos GC, Clough RW (1982): Further study of the earthquake response of a broad cylindrical liquid-storage tank model. *Earthquake Engineering Research Center Report No. UCB/EERC-82/07*, University of California at Berkeley.

[31] Haroun MA (1980): Dynamic analyses of liquid storage tanks. *Research Report California Institute of Technology, Pasadena, California, EERL 80-04*.

[32] Maley TJ, Roldán R, Lago A, Sullivan TJ (2012): *Effects of response spectrum shape on the response of steel frame and frame-wall structures*. IUSS Press, Pavia, Italy.

[33] CEN, European Committee for Standardisation. *ENV 1998-1, Eurocode 8. Design of structures for earthquake resistance – Part 1: General rules, seismic actions and rules for buildings*. Brussels, Belgium, 2005.

© The 17th World Conference on Earthquake Engineering